Metrol. Meas. Syst., Vol. 32 (2025), No. 4
DOI: 10.24425/mms.2025.155810

METROLOGY AND MEASUREMENT SYSTEMS
Index 330930, ISSN 0860-8229
www.metrology.wat.edu.pl

IMPROVEMENT OF THE PROCESS OF MEASURING THE DIMENSIONS OF PRECISION HOLES OF COMPLEX GEOMETRY

Serhii Kharchenko[1)], Sylwester Samborski[2)], Aleksander Czajka[2)], Michał Leleń[2)], Adam Wójtowicz[3),4)], Mariusz Kłonica[2)], Jakub Rzeczkowski[2)]

1) *Lublin University of Technology, Department of Applied Mechanics, Nadbystrzycka 38 D, 20-618 Lublin, Poland* (✉ *s.kharchenko@pollub.pl*)
2) *Lublin University of Technology, Department of Production Engineering, Nadbystrzycka 38 D, 20-618 Lublin, Poland*
3) *Central Office of Measures, Time and Length Metrology Department, Precise Geometric Measurements Laboratory, Elektoralna 2, 00-139 Warszawa, Poland*
4) *Cracow University of Technology, CUT Doctoral School, Faculty of Mechanical Engineering, Laboratory of Coordinate Metrology, al. Jana Pawła II 37, 31-864 Kraków, Poland*

Abstract

The industrial production of parts with precision holes for various applications requires high manufacturing accuracy. The dimensional verification of precision holes with complex geometry remains a critical challenge in modern manufacturing, particularly in ensuring reliability and process efficiency. Existing CMM procedures are largely optimized for circular holes and lack validated methodologies for complex-shaped apertures. A newl methodology for assessing the dimensional accuracy and inspection efficiency of epicycloid-shaped holes using CMMs is proposed: manufacturing surface samples with epicycloid-shaped holes using a Water Jet machine, conducting measurements on a ZEISS CONTURA CMM, optical validating measurement accuracy using microscopy on a Keyence VHX system and processing data through image segmentation of the hole, analyzing results and establishing dependencies of measurement accuracy and time on operational parameters. The dependencies of the mean deviation of epicycloid-shaped hole dimensions on the stylus movement speed and the number of measurement points have been established. Key findings indicate that stylus speed significantly influences measurement accuracy, while the number of probing points plays a secondary role. To address the limitations of conventional evaluation techniques, a new geometric complexity coefficient is proposed to quantify deviations from ideal shapes. This coefficient comprehensively characterizes deviations from the ideal geometric shape and includes the length of the curve forming the hole. The proposed methodology enables the optimization of measurement parameters for complex-shaped holes and improves inspection efficiency on industrial production lines. This approach contributes original insights into the metrological assessment of non-standard geometries, addressing a significant gap in existing literature.

Keywords: coordinate measuring machine, dimensional metrology, precision hole, accuracy and duration, measurement optimization.

1. Introduction

The quality of manufacturing many parts across various industries is determined by the geometric accuracy of precision holes: for bolted/riveted joints [1], splined connections [2], separation and filtration surfaces [3], and holes in rifled weapons barrels [4], as well as various technological equipment.

Numerous studies confirm that the precision of hole manufacturing directly affects the reliability of structural connections and technological efficiency of the equipment [5, 6]. In aviation, the reliability of bolted and riveted connections is partially determined by the geometric accuracy of hole manufacturing [1, 7]. Similarly, in industrial engineering, holes are used as anchor points for mounting parts [8]. The quality of separation of particles of loose

Article history: received April 24, 2025; revised September 23, 2025; accepted November 14, 2025; available online November 27, 2025.

materials is also determined by the accuracy of manufacturing holes of sifting surfaces, their geometric shape and periodic placement [9].

Holes with the standard (regular) geometric shape, for example round holes, do not always satisfy the requirements of modern technological equipment. The use of holes of *complex geometry* (CG) in the form of squares, hexagons, cycloidal shapes, *etc.*, allows to expand the potential capabilities of the equipment. One of the advantages is the possibility of increasing the contact area in the case of a connection, which improves the reliability of the equipment. An example is holes for spline joints in the form of: square spline fitting, triangular spline fitting, involute spline joint [2]. Another solution is the use of sifting surfaces with holes in the form of an epicycloid [10] or a Cassini oval shape [11] for the separation of loose materials, which can significantly (up to 100%) increase the completeness of the separation of particles due to the integration of irregularities on their surface. The accuracy of holes CG in press matrices also determines the quality of the final products of the raw material processing: granules, pellets, *etc.* [12, 13]. However, despite their growing importance, metrological methodologies for such shapes are insufficiently explored.

Work in this area is focused on improving manufacturing accuracy and measurement techniques through various approaches: optical systems [14], coordinate-based methods [15], hybrid optical-touch probes [16], ultrasonic sensors [17, 18], including using machine vision technologies [19].

Measuring techniques using the *coordinate measuring machines* (CMM) have become widespread in production lines. This method is based on spatial identification of the coordinates of an array of points on the test surface and subsequent data processing [20, 21]. The advantage of coordinate measurements is not only the direct measurement of individual (specified) points, but also the comparison of the obtained actual data with the original ones (*e.g.* CAD drawing) and the calculation of the necessary accuracy parameters (relative deviation, spatial placement of surfaces, *etc.*). Contact [22] and non-contact (optical) sensors [23, 24] can be used as a measuring element in a CMM.

Research and practical experience have allowed CMM manufacturers to create appropriate recommendations for the measurement method of hole sizes [21, 25], which relate only to the measurement of circle-shaped holes. Even modern CMM ZEISS CONTURA [25] offer only generalized guidelines for circular holes (for diameters <8 mm/8–25 mm – maximum stylus speed 3/5 mm/s; minimum number of points – 145/425; maximum tip diameter – 3 mm), without any validated procedures for CG holes.

One of the factors that ensure the accuracy of the measurement process is the magnitude of the error. Calibration of the measuring system allows you to reduce the magnitude of the error, for example, associated with mechanical wear of the measuring tip. The error in measuring the dimensions of parts by the CMM depends on the following factors: the state of the measuring system (reference system, accuracy corrections, *etc.*) [26], the state of the mechanical part of the measuring equipment (ensuring straightness and perpendicularity of the stylus movement, wear, *etc.*) [27], the influence of the external environment (temperature, humidity, vibrations, *etc.*) [28], the dynamic load of the measuring stylus (deformation or vibration of the rod) [29], the state of the measurement object (surface defects, shape deviations, roughness, *etc.*) [30], technological measurement modes (measurement plan, stylus speed, number of measurement points, stylus tip size, *etc.*) [31]. However, these are typically analyzed under assumptions of simple hole geometries.

To determine the error, it is necessary to conduct multiple experiments under the same conditions for one sample with one CMM. However, it should be noted that these results are subjective in relation to the type of sample. Their use is not universal and may be unjustified for other parts. This encourages the search for relative parameters that will allow for a comprehensive characterization of the shape of a hole CG during the measurement process.

The operating parameters of the CMM have a significant impact on the magnitude of the measurement error. Stępień, K. *et al.* [32], Gapinski, B. *et al.* [33] distinguish the following: the speed of the measured stylus tip, its dimensions (diameter), the number of measurement points, data processing parameters.

The time spent on identification is also a competitive indicator of measurement accuracy, which in general characterises the efficiency of the hole measurement process [34]. Minimizing measurement time is essential in industrial (mass) production of parts and technological lines with a significant number of operations, directly affecting economic profitability.

A critical synthesis of the reviewed sources indicates that most studies on hole quality in composites and alloys prioritize machining parameters rather than formalized metrological workflows [6, 7]. Optical approaches, including multi-camera and binocular-vision methods, attain high accuracy on circular apertures but their performance degrades on curved or epicycloidal profiles due to segmentation and edge-localization uncertainty [8, 19]. CMM remain the industrial reference, yet probing small radii and concave arcs tends to increase inspection time and uncertainty [20, 26, 32]. Hybrid tactile–optical systems enhance flexibility and traceability, but their implementation requires complex calibration and still lacks standardized integration in production environments [16]. Accordingly, the motivation of this work is to establish a structured, decision-driven measurement methodology that couples CMM probing with optical validation and formalizes parameter selection and feedback to meet both accuracy and throughput targets.

In light of the above, we conclude that there are no: - validated CMM-based measurement strategies for holes CG; studies on the influence of stylus speed and probing strategy on measurement accuracy; -methods to compare results across different CG profiles.

The aim of the research is to develop a methodology for measuring holes of complex geometry using CMMs, which includes optical validation, statistical data processing with optimisation for accuracy and measurement time, which fills a gap in standardised procedures for metrology of complex shapes.

To operationalize this aim, we adopt a modular workflow that integrates sample fabrication, standardized CMM setup and probing under controlled parameters, optical validation with automated image processing, computation of measurement characteristics, and regression-based modelling, with decision nodes enforcing accuracy and throughput requirements. This organization supports traceability and reproducibility in line with accepted practices in coordinate metrology [20, 26].

2. Methodology and materials

2.1. Materials

The object of the study was samples of perforated surfaces with holes in the form of an epicycloid, which is formed by the movement of a circle around a fixed circle (Fig. 1). A similar epicycloid shape, for simplification in practical serial production, can be decomposed into several curves of circles (10 pieces), which are interconnected (Fig. 1). Also, to determine the effect of a complex shape on the measurement process, the dimensions of typical round holes were investigated (R = 2.5/3/3.5mm).

The selected test geometry (Fig. 1) belongs to the family of planar cycloidal curves, which are characterized by periodic arrangement of local elements and symmetry with respect to the centre of the hole. These properties make the epicycloid a representative geometry for a broader class of complex contours, including algebraic and transcendental curves commonly found in engineering applications (Fig. 2).

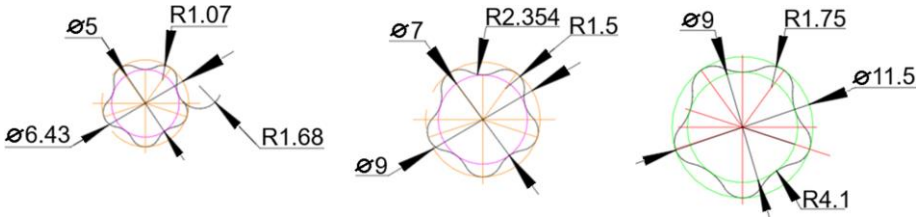

Fig. 1. Scheme of epicycloid-shaped holes.

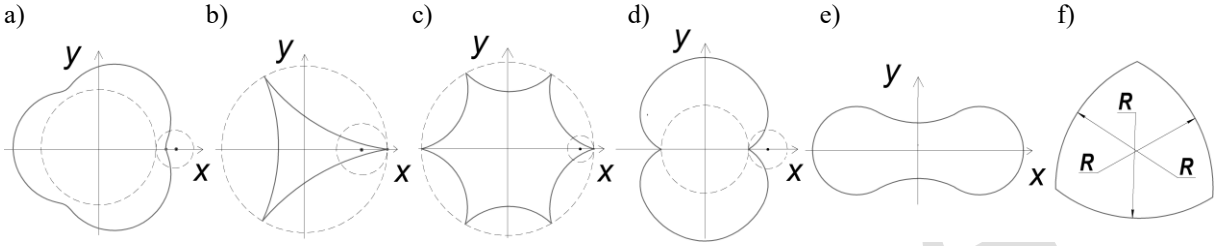

Fig. 2. Examples of algebraic and transcendental curves forming hole profiles: epitrochoid k=3 (a); deltoid k=3 (b); hypocycloid k=6 (c); nephroid k=2 (d); Cassini oval (e); Reuleaux triangle (f).

We will adopt the following terms in relation to the test holes (Fig.1) in accordance with the ISO 12181-1 [35]: r_1, r_2 – radiuses of circle: δ_n, δ_p – negative/positive local deviation.

For the production of precision holes CG, methods of cutting with an abrasive water jet under high pressure *abrasive water jet* (AWJ), were used. Industrial production of holes has significant advantages over manual in terms of duration, labor intensity, and quality [36].

The advantages of this method over others are [37]: the absence of additional equipment, the economic advantages of small-scale production, minimal deformation due to the low temperature and low pressure of the working jet, and the ability to process large parts.

The operating parameters of the machine are adopted in accordance with the machine operating instructions and the results of known studies [37, 38]: program pressure - 2500 bar; bulk material flow rate - 70%; compensation – 0.85 mm; head speed 500 mm/min, abrasive - Garnet mesh 80 E+. The sheet material chosen is steel S235JR with a thickness of 1 mm.

As a result, samples of perforated surfaces with epicycloid-shaped/round holes with a separation diameter of 5, 7 and 9 mm were manufactured (Fig. 3).

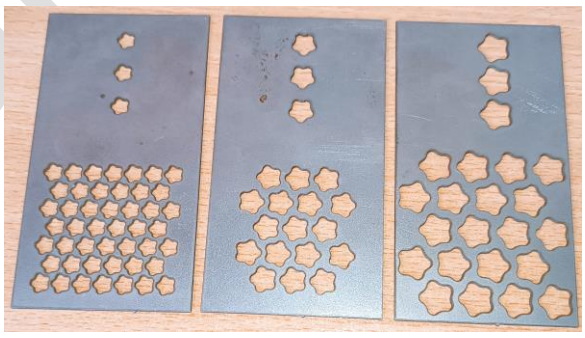

Fig. 3. General view of test samples of surfaces with holes of complex geometry.

2.2. Measuring equipment

To study the process of measuring the dimensions of precision holes, the CMM ZEISS CONTURA was used, which works according to the corresponding algorithm: probe and stylus calibration (determine the actual diameter of the stylus tip, orientation and length of the stylus); alignment process (transform the measurement coordinate system from the absolute coordinate

system or machine coordinate system of a CMM to part/workpiece coordinate system); design of a measurement strategy (reduce the distance of CMM axis movement, shorten the measurement time); data analysis (process data, in term of spatial coordinate points on a surface, from measurements); test and improvement of the measurement program (checking the correct operation of the program and the required results); measurement report design (determine the type of format of the report of a measurement to show).

The main measuring element of the CMM is a stylus with a tip in the form of a sphere. When measuring the dimensions, stylus touches the surface of the plane it will measure, fixing the coordinates of the specified points relative to the adopted coordinate system. For the studies, a stylus with parameters was selected: length 22mm, tip diameter 0,5mm.

The main technical characteristics of the CMM are as follows [39]: controller Type ZEISS C99m, Type according to ISO 10360-1:2000 – moving bridge CMM, relative humidity 40 % – 70%, ambient temperature 17 °C - 35 °C, operating mode – motorized / CNC, Sensor mounts – fixed installation, software – ZEISS CALYPSO, travel speed – motorized (axes) - 0 to 70 mm/s, acceleration (vector) – max. 1.85 m/s^2, measuring speed – max. 150 mm/s.

Regarding the measurement error for this CMM, we have [39] the length measurement error (ISO 10360-2) for 18 - 22 °C: E_l=1,5+L/ 350, where L – measurement length, mm. It should be noted that the presented determines the permissible maximum error for a specific stylus with a length of 60 mm and a ball diameter of 8 mm [40] and is also valid for the following configurations: Ø3×33mm; Ø5×50mm; Ø8×14mm; Ø12×92mm.

The adopted alignment of the measuring equipment with ISO specifications (measurement error length, stylus parameters, number of points and measurement speed) allows for successful integration of the results into other CMMs [20, 40], *e.g.*, Mitutoyo CRYSTA-Apex, Leitz Reference CMMs.

When calibrating the CMM, a calibration sphere was used, around which, at the recommended 25 points (from ISO 10360-2), measurements were performed with a stylus. The results were consistent with those allowed by the CMM specification, taking into account the measurement conditions [41]. The processing of measurement data is carried out using the Gaussian method, which has proven its adequacy [42]. Therefore, data processing was turned on and simultaneously excluded as an influence factor.

2.3. Methodology

The flowchart (Fig. 4) integrates sample fabrication, CMM setup and calibration, probing under defined parameters, and optical validation based on microscopy and image segmentation. The methodology incorporates modular computation of measurement characteristics, regression modelling, and sensitivity analysis of convex and concave arcs. Two decision nodes ensure compliance with accuracy and throughput requirements, while iterative feedback enables adaptive optimization. This representation emphasizes the structured and modular nature of the method, consistent with recent developments in vision-assisted metrology [43, 44].

According to the tasks of research on the CMM, the mode parameters varied: stylus speed v = 0.8/0.6/0.4/0.2 mm/s; the number of measurement points n = 200/300/400 pieces. The variation ranges were selected according to the recommendations of the CMM manufacturer and data of preliminary studies.

The criteria for effectiveness were the actual deviation from the nominal (CAD drawing) and the measurement time. The deviation of the entire hole was determined as the arithmetic mean of 10 curves (5 convex + 5 concave).

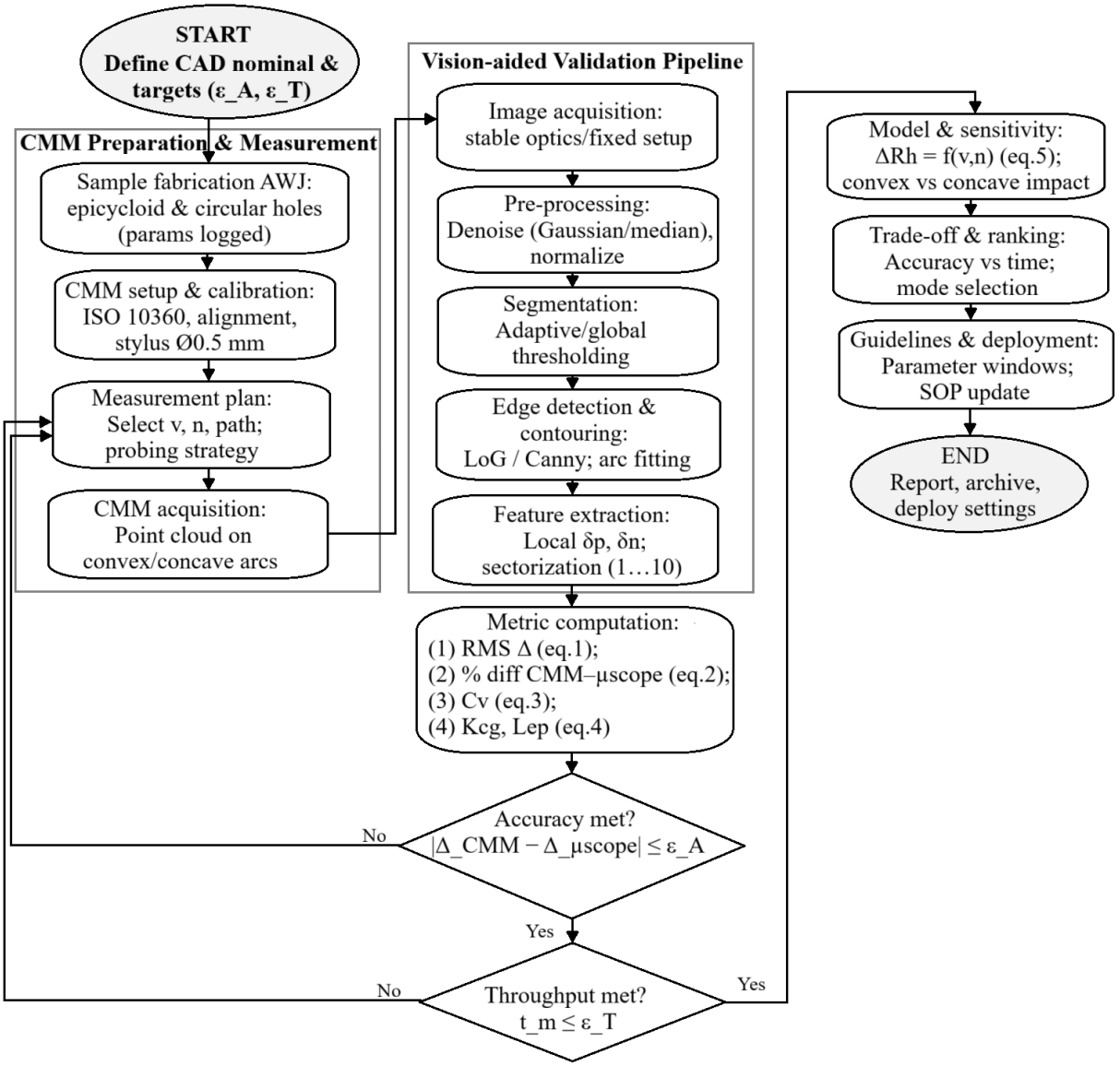

Fig.4. Flow chart of the proposed methodology for dimensional inspection of epicycloid-shaped holes.

An important stage of the study was the comparison of the results obtained from the CMM with a more accurate measurement method - microscopy. At this stage, the dimensions of holes CG were measured using a Keyence VHX 5000 Ver1.5.1.1 microscope with next parameters: shutter speed – auto 70, gain – present 0dB, Epi-illumination – on, scale width – 1 µm. Microscope was calibrated to ensure the required measurement accuracy.

To enhance methodological rigor, a dedicated validation protocol was implemented. First, all CMM-based measurements were systematically cross-verified with optical microscopy data acquired on the Keyence VHX system, providing an independent reference under ISO 10360 conditions. Second, the CMM calibration was performed with a certified reference sphere in accordance with ISO 10360-2, and compliance with the permissible error range was confirmed prior to each experimental series. Finally, reproducibility was assessed through repeated measurements under varied probing parameters (stylus speed and number of points), which demonstrated stable deviations across repetitions. These procedures collectively ensured traceability, ISO conformity, and experimental repeatability of the developed methodology.

The typical functionality of processing programs used with microscopes is not capable of measuring holes CG, in our case epicycloid. Dividing the test hole into curves (parts of circles) allows the use of radii (diameters) in the functionality of these programs.

For a complete analysis of the accuracy of CMM measurements under different operating conditions, it is necessary to have information about the deviation of the hole edge points from the CAD drawing. The image obtained from the microscope requires additional processing. To determine the deviation, we will carry out: sectorization of the image taking into account convex and concave circles (Fig. 5 a, b), uniform division of the curve of each sector into points and determination of the deviation, statistical processing using the Gaussian method and averaging over each sector, averaging data over the entire hole. Positive experience of dividing the image into sectors of round holes, further processing in the sector and averaging over the entire hole is given in [15]. Examples of the obtained hole images and their sectorization are presented in Fig. 6.

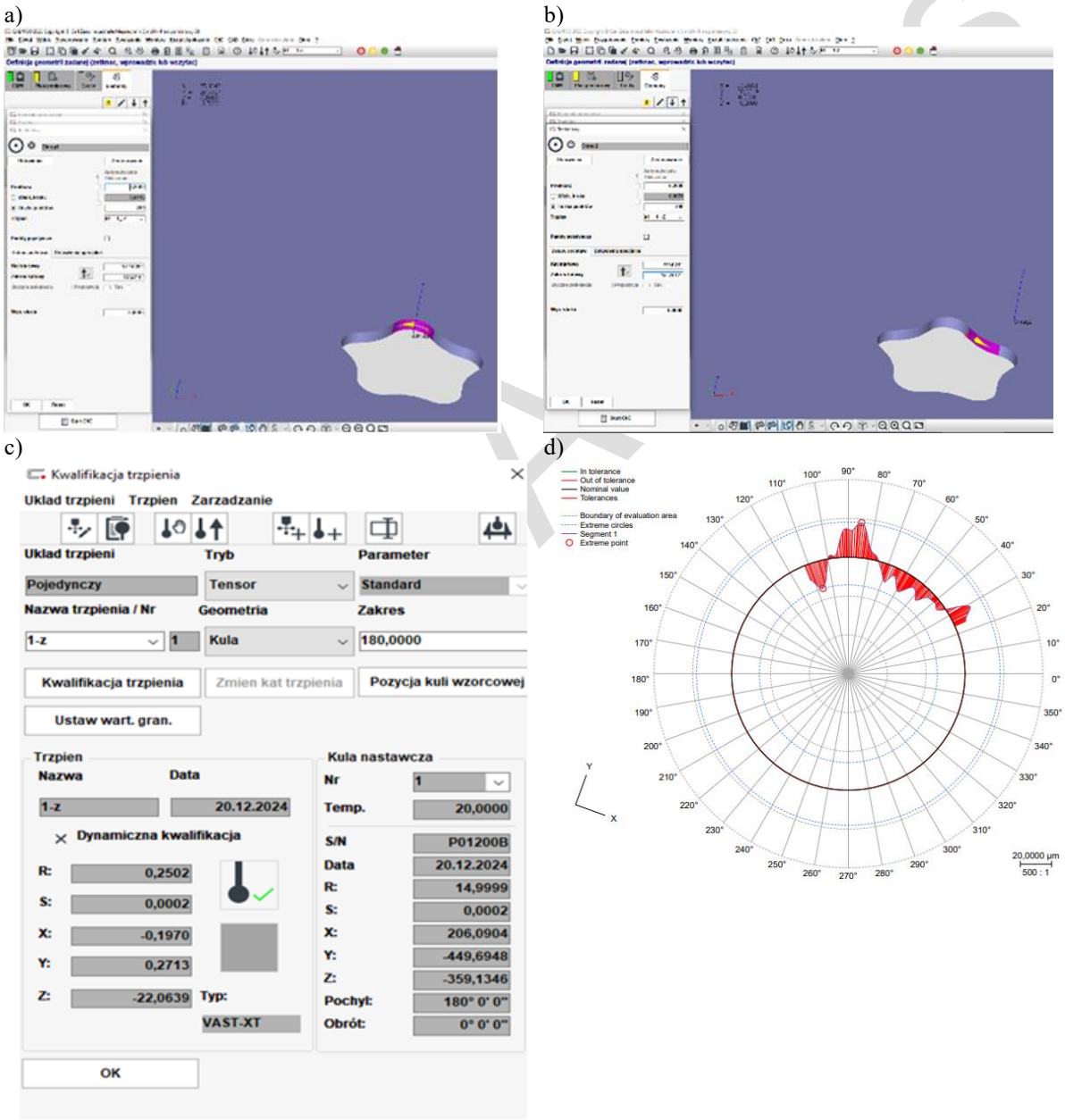

Fig. 5. Stages of the measurement process algorithm for the CMM: measurement plan of convex and concave parts of the hole circles (a, b); parameters during stylus calibration (c); visualization of measurement results (d).

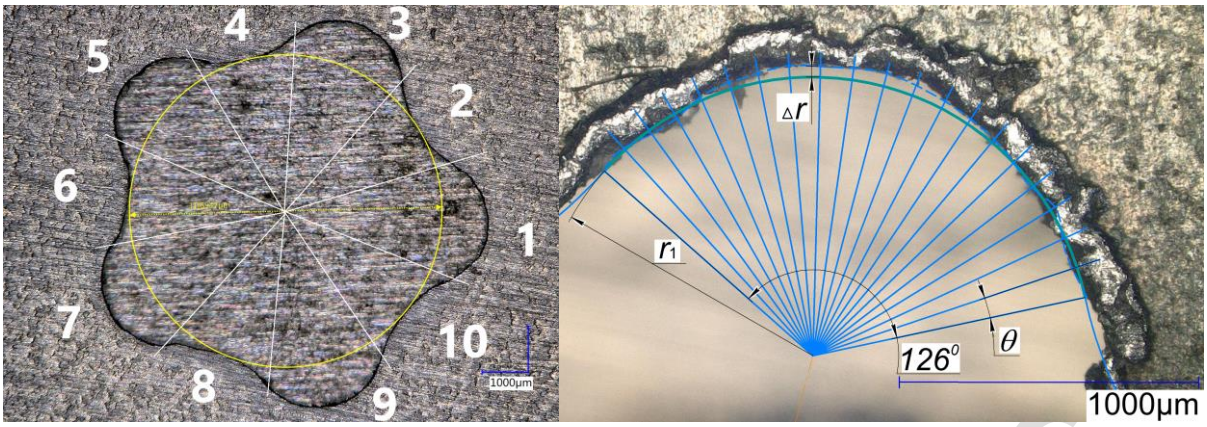

Fig. 6. Microscopy of holes and their sectorization by individual curves of circles (nr. 1…10).

The root-mean-square roundness deviation was determined by the equation [45]:

$$\Delta R_h = \sqrt{\frac{1}{2\pi}\int_0^{2\pi} \Delta r_i{}^2 d\theta}, \quad (1)$$

where Δr_i is the local roundness deviation, θ is the instantaneous angle in the roundness profile.

The obtained measurement data from CMM and microscopy were compared with each other, determining the absolute difference and percentage:

$$\varepsilon = \Delta R_{hmicro} - \Delta R_{h\mathrm{CMM}}, \varepsilon = \frac{\Delta \mathrm{R}_{hmicro}}{\Delta \mathrm{R}_{h\mathrm{CMM}}} 100\%, \quad (2)$$

where ΔR_{hmicro}– deviation of the dimensions of the entire hole obtained using microscopy, $\Delta R_{h\mathrm{CMM}}$ – deviation of the dimensions of the entire hole obtained using CMM.

A significant parameter that affects the productivity and quality of measurement is the length of the measurement object [46]. Measuring holes of complex geometry involves an increased curve length compared to the length of the curve of a typical circle.

The coefficient of variation (C_v) is an important parameter that defines the level of stability and accuracy of the measurements [47]:

$$C_v = \left(\frac{\sigma}{\mu}\right) \cdot 100\%, \quad (3)$$

where: σ – standard deviation; μ – average measurement value.

To account for the complexity of the hole geometry relative to the basic geometry (circle, rectangle, equilateral triangle), we introduce the corresponding geometry complexity coefficient K_{cg} [48]. The value of this coefficient equals the ratio of the curve length, which forms a hole CG, to the circumference length of the basic round hole [48]:

$$K_{cg} = L_{ep}/L_c = (k\frac{\pi}{180}(r_1\alpha_1 + r_2\alpha_2))/2\pi R, \quad (4)$$

where L_{ep}– length of the epicycloid curve (hole CG); L_c– length of the circle (basic hole); k – epicycloid multiplicity ($k = 5$); r_1, r_2 – radius of the convex and concave curves, respectively; α_1, α_2 – the angles that define the boundaries of the convex and concave curves, respectively. The use of this parameter makes it easier to analyze the measurement process data and provides a comprehensive assessment of the level of geometric complexity of the object. The K_{cg} coefficient serves as a complementary metric to ISO-based evaluations, offering a quantitative measure of intrinsic geometric variability in closed-loop profiles.

The proposed methodology can be successfully adapted to other CMMs or optical systems, provided that they meet key metrological requirements. Specifically, the CMM must support programmable point acquisition with controllable stylus speed and sufficient probing resolution

for non-circular contours. The optical system used for reference validation should offer a comparable level of magnification, field flatness, and pixel resolution to enable reliable segmentation and edge detection. Compatibility with ISO 10360 (for CMMs) and ISO 25178 (for surface imaging) ensures methodological consistency across platforms.

3. Results and discussion

The use of the developed method allowed us to obtain the dependence of the deviation (ΔR_h) of the sizes of epicycloid-shaped/round holes on the stylus speed and the number of measurement points (Fig. 7, Table 1, 2). The obtained deviations of the curves (Table 1) that form the hole of the epicycloid (k = 5)/round shapes, and their arithmetic mean is the deviation of the dimensions of the entire hole.

The results of the analysis of dependencies (Fig. 7, Table 1, 2) showed that the influence of the number of measurement points on the deviation value has a negligible effect (up to 3.1%).

Analyzing the results of measuring typical round holes (Table 2), we can note a slight variation in the values of the average deviation ($\Delta = \Delta R_{hCMmax} - \Delta R_{hCMmin}$ = 3.5-10.6 μm). The coefficients of variation of the data obtained are quite stable (up to 5%). This indicates the following: a) the influence of measurement modes on the accuracy is insignificant; b) the adequacy of the manufacturer's algorithms for compensating for deviations in the measurement process and recommendations for technological parameters, such as the speed of probe movement and the number of measurement points.

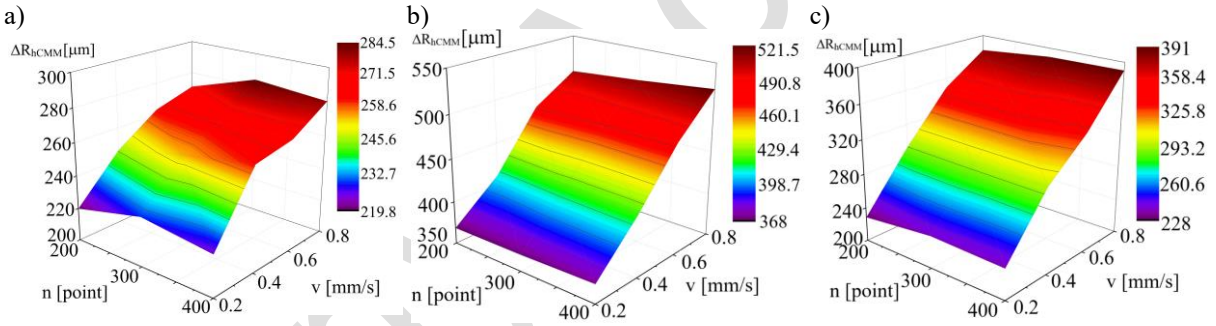

Fig. 7. Dependences of the deviation (ΔR_{hCMM}) of the sizes of holes on the stylus speed v and the number of measurement points n: (a) epicycloid-shaped hole (R = 2.5 mm; r_1 = 1.07 mm; r_2 = 1.65 mm; C_v = 8,5%); (b) epicycloid-shaped hole (R = 3.5 mm; r_1 = 1.5mm; r_2 = 2.35 mm; C_v = 11.6%); (c) epicycloid-shaped hole (R = 4.5mm; r_1 = 3.5mm; r_2 = 8.2 mm C_v = 15.7%).

The statistical justification for the study is presented in Table 3 and Fig. 8. The statistical data confirm and quantitatively assess the previous qualitative trends. For round holes, the average deviation monotonically decreases from 10.5 to 9.5 μm with increasing speed; the dispersion is small (SD ≈ 0.1 μm; CV ≈ 1%), indicating high repeatability of contact probing. For epicycloidal holes, the absolute deviations are larger and the dispersion is higher (SD ≈ 1.7–2.4 μm; CV ≈ 0.3–0.6%), which corresponds to the more demanding surface geometry. ANOVA reveals statistically significant differences between speed levels for both geometries (Table 2): $F(3,8) = 25.6$, $p = 0.0021$ (round); $F(3,8) = 158.4$, $p < 0.0001$ (epicycloidal). The corresponding effect sizes (η^2) are large, ≈ 0.91 and ≈ 0.98, respectively, indicating that stylus speed is the dominant factor influencing ΔR_h variability under the tested conditions, while the probing density (fixed at n = 300 points) does not significantly change the result.

Table 1. Patterns of change in the deviation of the curves forming an epicycloid-shaped hole (k = 5, R = 3.5 mm, r_1 = 1.5 mm, r_2 = 2.35 mm).

Nr.	Stylus speed v [mm/s]	Number of points n [pcs.]	Deviation [µm]										
			convex curves					concave curves					The entire hole ΔR_{hCM}
			circle 1	circle 3	circle 5	circle 7	circle 9	circle 2	circle 4	circle 6	circle 8	circle 10	
			Δr_1	Δr_3	Δr_5	Δr_7	Δr_9	Δr_2	Δr_4	Δr_6	Δr_8	Δr_{10}	
1	0.2	200	-80.5	67	105	-35.7	62	-189.5	963	-899.9	1887.4	260.7	368.4
2	0.2	300	-82.1	70.3	117.7	-32.3	63.9	-200.7	956	-901.7	1875.4	254.3	369.4
3	0.2	400	-80.5	71.1	130.1	-34.5	59.3	-191.6	106.2	-908.5	1886.3	251.2	371.93
4	0.4	200	-91	81	161	-50.1	69.5	-224.9	103.9	-932.5	2051.3	340.3	410.55
5	0.4	300	-89.4	82.8	181.7	-53.3	67	-223.9	95.7	-939.9	2106.6	333.9	417.42
6	0.4	400	-90	81.3	178.1	-52	65.7	-215.3	87.3	-938	2172.2	330.1	421
7	0.6	200	-96.6	94.4	218.9	-61.6	81.3	-239.6	119.5	-913.9	2547.7	392.2	476.57
8	0.6	300	-97.6	96.7	235.4	-63.6	82	-235.6	96.3	-920.1	2511.2	403	474.15
9	0.6	400	-96	96.4	241.4	-65.2	79.6	-225.3	96.4	-924.1	2581.6	385.3	479.13
10	0.8	200	-103.3	106.2	282.8	-65.5	92.4	-236	39.7	-884.7	2807	447.7	506.53
11	0.8	300	-106.5	108.3	279.4	-63.1	91.5	-210.5	64.5	-903.2	2880.8	423.1	513.09
12	0.8	400	-106.5	109.8	318.6	-62.3	92.8	-222.7	55.9	-896.3	2914.4	435.2	521.45

Table 2. Patterns of change in the duration (tm) and deviation (ΔR_{hCM}) of the typical round holes.

Nr.	Stylus speed v [mm/s]	Number of points n [pcs.]	R = 2.5 [mm]		R = 3.5 [mm]		R = 4.5 [mm]	
			ΔR_{hCM} [µm]	t_m [s]	ΔR_{hCM} [µm]	t_m [s]	ΔR_{hCM} [µm]	t_m [s]
1	0.2	200	29.2	82	10.80	114	28.7	148
2		300	28		10.50		28	
3		400	26.8		10.30		27.4	
4	0.4	200	25.5	41	10.20	57	26,3	74
5		300	26.4		10.20		27	
6		400	26.9		10.10		27.3	
7	0.6	200	26.2	28	9.80	38	25.5	48
8		300	26.4		9.80		26.7	
9		400	26.2		9.50		26	
10	0.8	200	25.1	20	9.50	28	25.2	37
11		300	25		9.50		26.1	
12		400	25.5		9.20		25.8	
Standard deviation SD, [µm]			1.45	-	0.48	-	1.01	-
Coefficient of variation CV, [%]			4.9	-	4.8	-	3.5	-

These findings align with recent metrology studies showing that traversal/scanning speed materially affects contact-based measurement performance (profilometry and CMM), and that replicate-based ANOVA is an appropriate method to evidence significance in dimensional metrology datasets [32, 49].

Taking into account the significant change in the duration of the measurement of round holes by varying the modes and the insignificant change in the deviation of dimensions, we can assert the expediency of using the mode: v = 0.8mm/s, n = 400 pcs.

A different trend is observed when studying holes CG. The stylus speed of the probe has the greatest influence in the epicycloid holes, which is: 23.2-24.8% (for hole R = 2.5mm), 37.5-40.2% (for hole R = 3.5mm), 64.1-67.2% (for hole R = 4.5mm). There is also a difference in the deviation value for convex and concave curves, where the latter exceed: 0.93-1.6 times (for

the hole $R = 2.5$mm), 5.5-8.5 times (for the hole $R = 3.5$mm), 1.8-2.5 times (for the hole $R = 4.5$mm). In our opinion, the change in the magnitude of the impact on the measurement accuracy is associated with the difference in the curvature (radius of rounding) and the length of the curves of the corresponding arcs or the measurement path. For practical use of the results, a regression equation was obtained that characterizes the change in the deviation of the epicycloid-shaped hole from the significant parameter - the stylus speed:

$$\Delta R_{hCMM} = -0.057X_1^2 + 0.301X_1 + 0.3102, \quad (5)$$

($R^2 = 0.997$) (for the hole $R = 3.5$mm).

As a result of the analysis, high values of the coefficient of variation ($C_v = 8.5$-15.7%) of the obtained data of the average deviation for holes of complex geometry were established. This proves the influence of measurement modes on accuracy indicators.

The above parameters, which characterize the difference from the correct geometry (in our case it is a circle), must be taken into account in the process of measuring holes CG.

The results of the next stage of research are presented in Table 4 in the form of a more accurate measurement method for experimental holes - microscopy.

Table 3. Statistical summary of deviations ΔR_h for round and epicycloid holes ($R = 3.5$ mm, n = 300 pcs.)

Geometry	**Stylus speed v [mm/s]**	**Deviation (repetitions) [µm]**	**Mean deviation ΔR_h [µm]**	**Standard deviation SD [µm]**	**Coefficient of variation CV [%]**	**ANOVA F**	**ANOVA *p*-value**
Round hole	0.2	10.4	10.50	0.1	0.95	25.6	0.0021
		10.5					
		10.6					
	0.4	10.2	10.2	0.1	0.98		
		10.1					
		10.3					
	0.6	9.7	9.8	0.1	1.02		
		9.8					
		9.9					
	0.8	9.6	9.5	0.1	1.05		
		9.4					
		9.5					
Epicycloid hole	0.2	367	369.4	2.35	0.64	158.4	< 0.0001
		369.5					
		371.7					
	0.4	415	417.4	2.35	0.56		
		417.6					
		419.7					
	0.6	474.8	474.2	2.4	0.51		
		472					
		476.8					
	0.8	511	513.1	1.71	0.33		
		514.2					
		513.9					

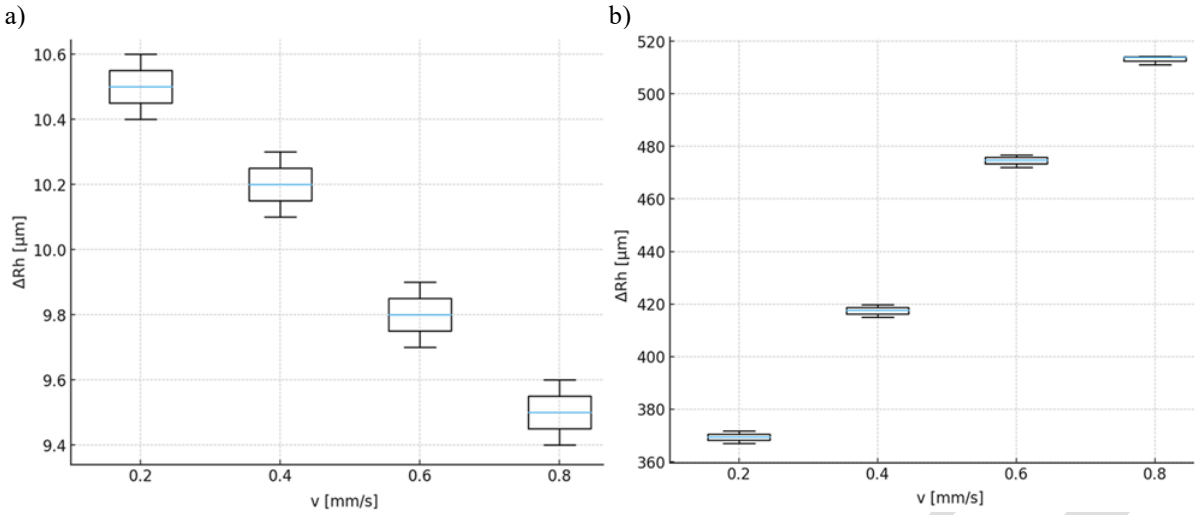

Fig.8. Boxplot of deviations ΔR_h for round (a) and epicycloid (b) holes grouped by stylus speed v (R = 3.5 mm).

Table 4. Microscopy of epicycloid-shaped holes.

Hole size [mm]	**Average deviation [μm]**										
	circle 1	**circle 3**	**circle 5**	**circle 7**	**circle 9**	**circle 2**	**circle 4**	**circle 6**	**circle 8**	**circle 10**	**The entire hole $\Delta R_{h\ micro}$ [μm]**
R	Δr_1	Δr_3	Δr_5	Δr_7	Δr_9	Δr_2	Δr_4	Δr_6	Δr_8	Δr_{10}	
2.5	35.1	206.3	78	150.2	71.4	276.8	281.5	-283.5	281.6	324.2	191.84
3.5	25	163	-12	-50.1	69.5	135	-172	-157	2051.3	340.3	317.52
4.5	-95.9	37.1	-121.5	-204.3	73.8	76.2	-301.8	82.18	37.9	-294.6	206.49

Sectoring of curves and identification of local deviations from the CAD-drawing on the image allowed to establish the corresponding deviations and calculate the average deviation for the entire hole ($\Delta R_{h\ micro}$).

Comparison of the aperture deviation obtained by microscopy with the deviations obtained with CMM (for 13 different modes) allowed us to determine the absolute and relative difference between the methods (Fig. 9, 10).

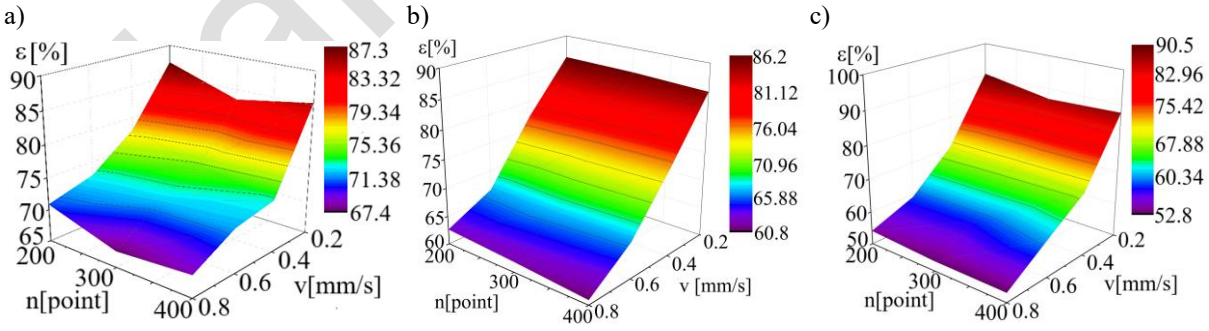

Fig. 9. Accuracy of hole measurements on the CMM compared to microscopy, depending on the number of measurement points and the stylus movement speed: (a) hole R = 2.5 mm (k=5, r_1 = 1.07 mm, r_2 = 1.65 mm); (b) hole R = 3.5 mm (k = 5, r_1 = 1.5mm, r_2 = 2.35 mm); (c) hole R = 4.5mm (k = 5, r_1 = 3.5mm, r_2 = 8.2 mm).

Metrol. Meas. Syst., Vol. 32 (2025), No. 4
DOI: 10.24425/mms.2025.155810

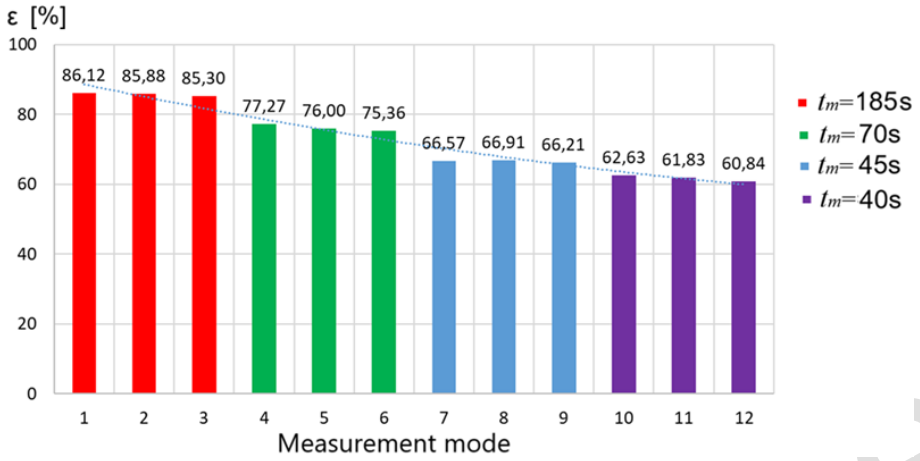

Fig. 10. Measurement accuracy and duration of hole dimensions on the CMM across different modes (R = 3.5 mm).

Using the obtained data, the measurement process modes were ranked according to the accuracy criterion (difference between the methods). One of the options when using CMM is the automatic identification of the time spent on the measurement process, which was indicated according to the modes in the studies of epicycloid-shaped holes (Fig. 9, 10) and standard round holes (Table 2).

The analysis of dependencies (Fig. 9, 10) showed that the measurement accuracy decreases by 25.3%-37.6% when using the mode with the highest (in the experimental range) stylus measuring speeds (0.8 mm/s). However, as noted earlier, the recommendations of the CMM manufacturer are limited by the limit values [25]: the maximum probe measuring speed (v = 3 mm/s) and the minimum number of measurement points (145). The second important criterion is the measurement accuracy, which, as can be seen from the data (Fig.10), significantly depends on the selected mode. According to the studied modes, the change in measurement time on a given CMM occurs by 4.6 times. This significantly differs from the stable measurement time of typical round holes (Table 2).

The agreement between CMM results and optical microscopy (Fig. 9, 10) substantiates the validity of the developed approach. The consistent convergence of both methods across multiple repetitions confirms that the methodology is not only robust against parameter variations but also reproducible under industrially relevant conditions. This dual verification provides strong evidence of methodological soundness.

As we can see, the lack of scientifically based recommendations and limited data from CMM manufacturers regarding the modes of the process of measuring holes CG leads to a loss of accuracy and an increase in the duration of measurement. This significantly affects the technological and economic efficiency of manufacturing of parts with precision holes.

To confirm the results, additional studies were conducted to measure the sizes of epicycloid-shaped holes that have a different standard size (for sifting surfaces - the main separation diameter or radius R). Using the developed methodology, size deviations were obtained depending on the main hole size (R) and the stylus speed (Fig. 11). At the same time, the number of measurement points, as an insignificant factor, was fixed at n = 300 points.

Analysis of the results (Fig. 11) shows that despite the increase in the size of the hole, the identity of the change in measurement accuracy depending on the stylus speed remains. Varying the main size of the hole leads to a change in the deviation of the hole by 3.3-80.5%, which indicates a difference in the measurement path or the length of the hole contour curve.

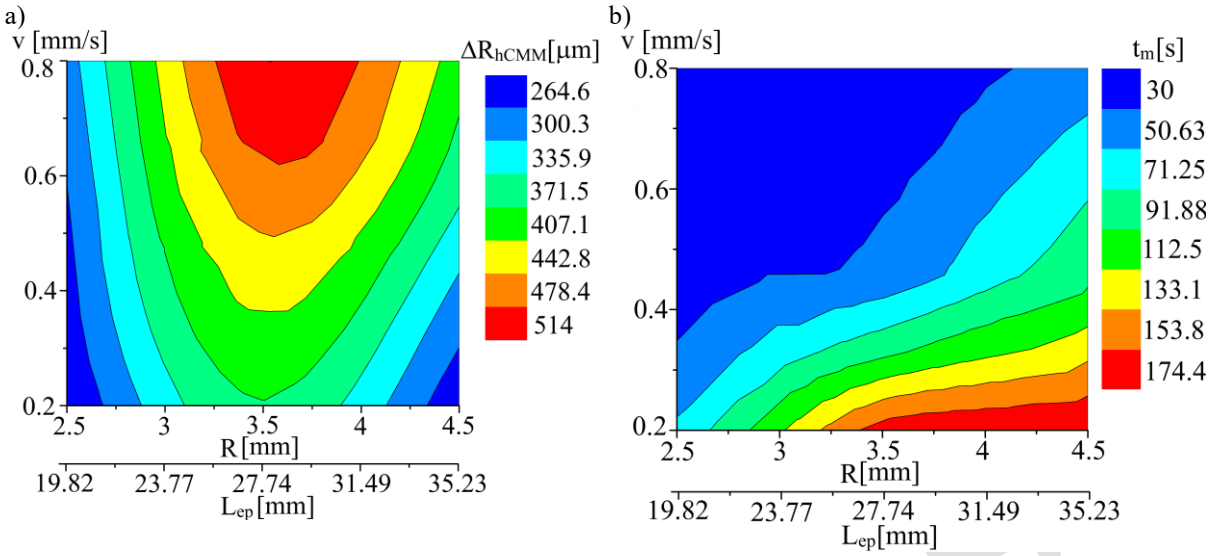

Fig. 11. Dependences of the efficiency of the hole measurement process on its main size (R) and the length of the contour curve (L_{ep}), the stylus measuring speed (v): accuracy (a), duration (b) (K_{cg} = 1.26; n = 300 points).

To be able to disseminate the research results, it is necessary to move from absolute to relative parameters of holes that comprehensively characterize the shape of complex geometry. Taking into account the research data, such parameters were the length of the hole contour curve and the geometry complexity coefficient, which were obtained for the experimental holes (Fig. 11). For a given hole geometry (Fig. 1), the value of the geometry complexity coefficient K_{cg} is in the range of 1.24 ... 1.26.

The presented data form (Fig.11) is more universal, because it can be used for recommendations on the modes of the measurement process on the CMM of holes with any geometry that differs from the correct shape (circle, triangle, rectangle). A comprehensive representation of the complexity of the hole shape involves characterizing: the measurement path as the length of the curve L_{ep}, and the complexity (curvilinearity) as a coefficient K_{cg}. The results demonstrate that increasing stylus speed has a stronger negative impact on accuracy than reducing the number of points, indicating that optimization should prioritize stable motion over point density. These findings provide a foundation for minimizing inspection cycle time without significantly compromising precision. Future work will include a quantitative cost-efficiency model that accounts for equipment wear, computational load, and operator time to support practical implementation.

Although the present study is focused on holes with epicycloid-shaped profiles, the developed measurement methodology can be effectively applied to other geometries as well (Fig. 2). The similarity in metrical characteristics, particularly the variability of curvature and closed-loop periodicity, supports the applicability of the proposed method and its potential to improve measurement quality for such shapes using CMMs.

With regard to the industrial validation of the developed methodology, it should be noted that additional measurement uncertainty may arise due to adverse high-throughput conditions, including thermal drift, structural vibrations, operator variability, *etc.* A positive aspect of the proposed measurement concept is its modular nature, which allows for integration into inspection systems equipped with compensation algorithms for mitigating adverse influences.

4. Conclusions

1. This study presents a validated methodology for the dimensional inspection of holes with complex geometry, using a CMM and microscopy for cross-verification. The main components

of the developed methodology include: fabrication of perforated surface samples with epicycloid-shaped holes using a Water Jet machine; measurement on a ZEISS CONTURA CMM under predefined operating parameters; verification of measurement adequacy through microscopy with a Keyence VHX system and data processing with hole image segmentation; analysis of results and determination of the relationship between measurement accuracy and duration with CMM operating parameters; identification of complex parameters characterizing the hole geometry.

2. The influence of stylus speed and probing density on roundness accuracy and measurement time was systematically evaluated. It was shown that increased stylus speed significantly affects measurement error, whereas the number of probing points has a secondary influence, enabling process time reduction without compromising precision. The ranking made it possible to establish the regularity of the change in the measurement accuracy and duration for 12 CMM measurement modes, providing recommendations for the industrial use for measuring holes of complex geometry.

3. Statistical evaluation with repetitions and ANOVA confirmed a significant influence of probe speed on roundness deviation ($p < 0.05$). It was also found that circular holes have high repeatability (CV ≈ 1%), while epicycloidal holes have greater variation (CV up to 0.6%) due to their geometric complexity.

4. A novel metric, the geometric complexity coefficient, was introduced to characterize the internal geometric variability of closed contours. This coefficient serves as a supplementary criterion to ISO-based form deviation assessments and supports enhanced analysis of complex shapes beyond standard circular features.

5. The modular structure of the methodology ensures its adaptability to other ISO-compliant CMMs and optical platforms, with future work planned for cross-system validation under industrial conditions. These findings contribute to the advancement of geometric inspection strategies for complex-featured components and offer a pathway toward standardized dimensional control beyond circular geometries. Moreover, the methodology has undergone explicit validation through cross-verification with optical microscopy, ISO-based calibration procedures, and reproducibility testing under varied measurement modes. These elements confirm that the proposed approach yields traceable, standardized, and reliable results, thereby enhancing its practical applicability for industrial inspection systems.

Reference

[1] Qi, Z., Liang, G., Dai, Y., Qiu, J., & Hao, H. (2023). The effects of countersink depth on fatigue performance of CFRP joint. *Research Square (Research Square)*. https://doi.org/10.21203/rs.3.rs-3080254/v1

[2] Bodzás, S. (2020). Manufacturing of the surfaces of spline fitting connection. *The International Journal of Advanced Manufacturing Technology*, *111*(3–4), 909–920. https://doi.org/10.1007/s00170-020-06194-w

[3] Kharchenko, S., Kovalishin, S., Zavgorodniy, A., Kharchenko, F., & Mikhaylov, Y. (2019). Effective sifting of flat seeds through sieve. *INMATEH Agricultural Engineering*, *58*(2), 17–26. https://doi.org/10.35633/INMATEH-58-02

[4] Shen, C., Zhou, K., Lu, Y., & Li, J. (2019). Modeling and simulation of bullet-barrel interaction process for the damaged gun barrel. *Defence Technology*, *15*(6), 972–986. https://doi.org/10.1016/j.dt.2019.07.009

[5] Ahmed, A., Lew, M., Diwakar, P., Kumar, A. S., & Rahman, M. (2019). A novel approach in high performance deep hole drilling of Inconel 718. *Precision Engineering*, *56*, 432–437. https://doi.org/10.1016/j.precisioneng.2019.01.012

[6] Biruk-Urban, K., Bere, P., Udroiu, R., Józwik, J., & Beer-Lech, K. (2024). Understanding the effect of drilling parameters on hole quality of Fiber-Reinforced polymer structures. *Polymers*, *16*(16), 2370. https://doi.org/10.3390/polym16162370

[7] Aamir, M., Giasin, K., Tolouei-Rad, M., & Vafadar, A. (2020). A review: drilling performance and hole quality of aluminium alloys for aerospace applications. *Journal of Materials Research and Technology*, *9*(6), 12484–12500. https://doi.org/10.1016/j.jmrt.2020.09.003

[8] Tao, L., Xia, R., Zhao, J., Zhang, T., Li, Y., Chen, Y., & Fu, S. (2022). A high-accuracy circular hole measurement method based on multi-camera system. *Measurement*, *207*, 112361. https://doi.org/10.1016/j.measurement.2022.112361

[9] Kharchenko, S., Samborski, S., Kharchenko, F., Korzec-Strzałka, I., & Andrii, A. S. (2024). Dynamics of Loose Materials and Oscillations of Cylindrical Perforated Sifting Surfaces with Volumetric Riffles. *Advances in Science and Technology – Research Journal*, *18*(8), 238–255. https://doi.org/10.12913/22998624/194114

[10] Bakum, M., Kharchenko, S., Kovalyshyn, S., Krekot, M., Kharchenko, F., Shvets, O. P., Kiełbasa, P., & Miernik, A. (2022). Identification of parameters of the separation process of safflower seed material on sieves. *Journal of Physics Conference Series*, *2408*(1), 012013. https://doi.org/10.1088/1742-6596/2408/1/012013

[11] Bredykhin, V., Tikunov, S., Slipchenko, M., Alfyorov, O., Bogomolov, A., Shchur, T., Kocira, S., Kiczorowski, P., & Paslavskyy, R. (2023). Improving efficiency of corn seed separation and calibration process. *Agricultural Engineering/Inżynieria Rolnicza*, *27*(1), 241–253. https://doi.org/10.2478/agriceng-2023-0018

[12] Mitrus, M., Tydman, K., Milanowski, M., Soja, J., Lewko, P., Kupryaniuk, K., & Wójtowicz, A. (2024). Influence of the forming die design on processing and physical properties of Gluten-Free crisps. *Agricultural Engineering/Inżynieria Rolnicza*, *28*(1), 87–96. https://doi.org/10.2478/agriceng-2024-0007

[13] Nielsen, S. K., Mandø, M., & Rosenørn, A. B. (2019). Review of die design and process parameters in the biomass pelleting process. *Powder Technology*, *364*, 971–985. https://doi.org/10.1016/j.powtec.2019.10.051

[14] Wang, P., Kong, L., An, H., Gao, M., & Cui, H. (2023). Fast and accurate measurement of hole systems in curved surfaces. *Photonics*, *10*(12), 1337. https://doi.org/10.3390/photonics10121337

[15] Meng, F., Yang, J., Yang, G., Lu, H., Dong, Z., Kang, R., Guo, D., & Qin, Y. (2024). A visual measurement method for deep holes in composite material aerospace components. *Sensors*, *24*(12), 3786. https://doi.org/10.3390/s24123786

[16] Gąska, A., Gąska, P., Gruza, M., Harmatys, W., Kowaluk, T., Styk, A., Jakubowicz, M., Wójtowicz, A., Wiśniewski, M. A., & Sładek, J. (2024). Traceability Assurance method for measurements performed using hybrid measuring systems consisting of tactile and optical devices. *Advances in Science and Technology – Research Journal*, *18*(7), 447–459. https://doi.org/10.12913/22998624/193736

[17] Caggiano, A., & Nele, L. (2018). Comparison of drilled hole quality evaluation in CFRP/CFRP stacks using optical and ultrasonic non-destructive inspection. *Machining Science and Technology*, *22*(5), 865–880. https://doi.org/10.1080/10910344.2018.1466330

[18] Samborski, S., Rzeczkowski, J., & Korzec-Strzałka, I. (2023). Experimental study of delamination process in elastically coupled laminates with the acoustic emission technique. *Engineering Structures*, *300*, 117196. https://doi.org/10.1016/j.engstruct.2023.117196

[19] Xia, R., Su, R., Zhao, J., Chen, Y., Fu, S., Tao, L., & Xia, Z. (2019). An accurate and robust method for the measurement of circular holes based on binocular vision. *Measurement Science and Technology*, *31*(2), 025006. https://doi.org/10.1088/1361-6501/ab4ed5

[20] Phillips, S. (2011), *Performance Evaluations, Coordinate Measuring Machines and Systems* (2nd ed.). CRC Press, Boca Raton, FL

[21] Sładek, J. (2011), Accuracy of coordinate measurements. Publishing House of Cracow University of Technology, Cracow

[22] Chen, B., Zhang, X., Zhang, H., He, X., & Xu, M. (2013). Investigation of error separation for three dimensional profile rotary measuring system. *Measurement*, *47*, 627–632. https://doi.org/10.1016/j.measurement.2013.09.043

[23] Liu, L., Zhang, H., Jiao, F., Zhu, L., & Zhang, X. (2023). Review of optical detection technologies for inner-wall surface defects. *Optics & Laser Technology*, *162*, 109313. https://doi.org/10.1016/j.optlastec.2023.109313

[24] Zhao, Y., Zhao, H., Lv, R., & Zhao, J. (2019). Review of optical fiber Mach–Zehnder interferometers with micro-cavity fabricated by femtosecond laser and sensing applications. *Optics and Lasers in Engineering*, *117*, 7–20. https://doi.org/10.1016/j.optlaseng.2018.12.013

[25] Zeiss Academy Metrology. Cookbook. Strategie pomiarowe w pomiarach metodą stykową. Carl Zeiss Industrielle Messtechnik GmbH, Germany. 2019. 165p.

[26] Poniatowska, M. (2011). Parameters for CMM contact measurements of Free-Form surfaces. *Metrology and Measurement Systems*, *18*(2), 199–208. https://doi.org/10.2478/v10178-011-0003-z

[27] Matuszak, J., Klonica, M., & Zagorski, I. (2019). Effect of Brushing Conditions on Axial Forces in Ceramic Brush Surface Treatment. In *IEEE 5th International Workshop on Metrology for AeroSpace,* 644–648. https://doi.org/10.1109/metroaerospace.2019.8869605

[28] Sur, A., Bhatkar, V. W., & Roy, A. (2022). Effect of term of error on wet bulb temperature measurement using aspiration psychrometer. *Frontiers in Heat and Mass Transfer*, *19,* 1-8. https://doi.org/10.5098/hmt.19.3

[29] Muralikrishnan, B., Stone, J., & Stoup, J. (2005). Fiber deflection probe for small hole metrology. *Precision Engineering*, *30*(2), 154–164. https://doi.org/10.1016/j.precisioneng.2005.07.004

[30] Woźniak, A., & Dobosz, M. (2005). Influence of measured objects parameters on CMM touch trigger probe accuracy of probing. *Precision Engineering*, *29*(3), 290–297. https://doi.org/10.1016/j.precisioneng.2004.11.009

[31] Magdziak, M., & Ratnayake, R. C. (2018). Investigation of best parameters' combinations for coordinate measuring technique. *Procedia CIRP*, *78*, 213–218. https://doi.org/10.1016/j.procir.2018.08.173

[32] Stepien, K., Kmiecik-Sołtysiak, U., Cepova, L., & Zuperl, U. (2024). Problems of measurements of roundness deviations with the use of coordinate measuring machines. *MM Science Journal*, *2024*(1). https://doi.org/10.17973/mmsj.2024_02_2023142

[33] Gapinski, B., & Rucki, M. (2008). The roundness deviation measurement with CMM. In *IEEE International Workshop on Advanced Methods for Uncertainty Estimation in Measurement*. 108-111. https://doi.org/10.1109/amuem.2008.4589944

[34] Mian, S. H., & Al-Ahmari, A. (2013). Enhance performance of inspection process on Coordinate Measuring Machine. *Measurement*, *47*, 78–91. https://doi.org/10.1016/j.measurement.2013.08.045

[35] ISO 12181-1:2011. Geometrical product specifications (GPS) – Roundness – Part 1: Vocabulary and parameters of roundness.

[36] Bi, S., & Liang, J. (2010). Robotic drilling system for titanium structures. *The International Journal of Advanced Manufacturing Technology*, *54*(5–8), 767–774. https://doi.org/10.1007/s00170-010-2962-2

[37] Krajcarz, D. (2014). Comparison Metal Water Jet Cutting with Laser and Plasma Cutting. *Procedia Engineering*, *69*, 838–843. https://doi.org/10.1016/j.proeng.2014.03.061

[38] Bławucki, S., Zaleski, K., & Leleń, M. (2016). Analysis of capabilities of cutting thin-walled structures of EN AW-2024 T351 alloy using an abrasive water-jet. *Mechanik*, *8–9*, 1078–1079. https://doi.org/10.17814/mechanik.2016.8-9.256

[39] ZEISS CONTURA. Specifications. Carl Zeiss Industrielle Messtechnik GmbH. Version: 2021-05. 7 p.

[40] Ratajczyk, E. (2017). New types of coordinate measuring machines and symbols used for their parameters. Part II: Examples of gantry machines. *Mechanik*, *5–6*, 462–467. https://doi.org/10.17814/mechanik.2017.5-6.61

[41] Arenhart, R. S., Pizzolato, M., Beuren, F. H., Souza, A. M., & Da Rosa, L. C. (2021). Device for interim check of coordinate measuring machines. *Metrology and Measurement Systems*, 143–158. https://doi.org/10.24425/mms.2022.138546

[42] Sun, L., Ren, M., & Yin, Y. (2017). Domain-specific Gaussian process-based intelligent sampling for inspection planning of complex surfaces. *International Journal of Production Research*, *55*(19), 5564–5578. https://doi.org/10.1080/00207543.2017.1301688

[43] Saif, Y., Yusof, Y., Latif, K., Kadir, A. Z. A., Ahmed, M. B. L., Adam, A., Hatem, N., & Memon, D. A. (2022). Roundness Holes' Measurement for milled workpiece using machine vision inspection system based

on IoT structure: A case study. *Measurement*, *195*, 111072. https://doi.org/10.1016/j.measurement.2022.111072

[44] Yıldırım, Ş., Çabuk, N., & Bakırcıoğlu, V. (2023). Experimentally flight performances comparison of octocopter, decacopter and dodecacopter using universal UAV. *Measurement*, *213*, 112689. https://doi.org/10.1016/j.measurement.2023.112689

[45] Muralikrishnan, B., & Raja, J. (2008). *Computational surface and roundness Metrology*. https://doi.org/10.1007/978-1-84800-297-5

[46] Cuesta, E., Alvarez, B., Sanchez-Lasheras, F., & Gonzalez-Madruga, D. (2015). A statistical approach to prediction of the CMM drift behaviour using a calibrated mechanical artefact. *Metrology and Measurement Systems*, *22*(3), 417–428. https://doi.org/10.1515/mms-2015-0033

[47] Crowder, S., Delker, C., Forrest, E., & Martin, N. (2020). *Introduction to Statistics in Metrology*. https://doi.org/10.1007/978-3-030-53329-8

[48] Kharchenko, S., Samborski, S., Paśnik, J., & Kharchenko, F. (2024). The natural oscillations of perforated sifting surfaces with epicycloidal holes. *Advances in Science and Technology – Research Journal*, *19*(1), 256–268. https://doi.org/10.12913/22998624/195463

[49] Urban, J., Beranek, L., Koptiš, M., Šimota, J., & Košťák, O. (2020). Influence of CMM scanning speed and inspected feature size on an accuracy of size and form measurement. *Manufacturing Technology*, *20*(4), 538–544. https://doi.org/10.21062/mft.2020.074

Serhii Kharchenko Assoc. Prof. DSc PhD Eng, is a Professor at the Department of Applied Mechanics, Faculty of Mechanical Engineering, LUT (Poland). He earned his PhD (2007) and DSc (2018) degrees. Member of the Polish Society of Theoretical and Applied Mechanics. Interests: mechanics of materials; dynamics of loose media; damage identification; numerical simulations. Author of more than 10 monographs, 22 patents, 140 publications.

Sylwester Samborski, Assoc. Prof. DSc PhD Eng. is the Head of the Department of Fundamentals of Production Engineering. He defended his PhD thesis in the discipline of machine construction and maintenance in 2006 at LUT. He obtained his DSc degree from Lodz University of Technology in 2018. Since 2020, he holds the position of Vice-Dean at the Faculty of Mechanical Engineering of LUT. Author of more than 60 articles, numerous inventive projects *etc.* His interests are broadly understood mechanical engineering, signal analysis, metrology.

Adam Wójtowicz graduated in theoretical physics from the University of Warsaw. He is currently Chief Metrologist at the Central Office of Measures, working in the Laboratory of Precision Geometric Measurements. He is associated with the Doctoral School of the Cracow University of Technology, Laboratory of Coordinate Metrology. He has participated in international research projects within the EMPIR and EPM programs, focusing on digital metrology twins and uncertainty in coordinate measurements. He has co-authored several scientific publications in applied metrology. His current interests include digital metrology, measurement uncertainty evaluation and coordinate measurement techniques.

Aleksander Czajka is a PhD student at LUT and an employee of the Department of Fundamentals of Production Engineering. His current research area is application of machine learning in metrology and application of acoustic emission in damage detection of CFRP composites.

Michał Leleń received his master's degree from the LUT. He is currently a specialist at the Department of Production Engineering Fundamentals at the LUT. He is the co-author of several publications in journals and at conferences. His interests include production, AWJ and CNC machining.

Mariusz Kłonica received the Ph.D. degree from Lublin University of Technology, Poland, in 2015. He has authored or coauthored 1 books, 25 book chapters, over 70 journal and 30 conference publications. He holds 5 issued patents. His current research interests include CMM, machine technologies, and material strength.

Jakub Rzeczkowski obtained a Ph.D. degree. He is currently an assistant professor at the Faculty of Mechanical Engineering in the LUT. He has coauthored over 12 journal and conference publications. His interests include delamination in composite laminates, application of acoustic emission technique, machine learning algorithms and numerical modelling.